International Journal of Mass Spectrometry xxx (2015) xxx–xxx

Contents lists available at ScienceDirect

International Journal of Mass Spectrometry

journal homepage: www.elsevier.com/locate/ijms

Mass spectral study of the occurrence of tautomeric forms of selected enaminones

Q1 Danila L. Ruiz, Agustín Spaltro, Maricel Caputo, Dacio A. Iglesias, Patricia Ercilia Allegretti*

Laboratorio de Estudio de Compuestos Orgánicos (LADECOR), Departamento de Química, Facultad de Ciencias Exactas, Universidad Nacional de La Plata, 47 y 115, 1900 La Plata, Buenos Aires, Argentina

ARTICLE INFO

Article history:
Received 21 August 2014
Received in revised form 5 December 2014
Accepted 19 December 2014
Available online xxx

Keywords:
Enaminones
Tautomerism
Mass spectrometry

ABSTRACT

The mass spectra of enaminones can provide valuable information with regards to tautomeric equilibria in the gas phase. Mass spectra of selected enaminones have been analyzed and specific fragmentation assignments have been done to characterized and weigh co-existing all possible tautomers of enaminones. Thioenaminones are of particular interest due to their tendency to shift the tautomeric equilibrium towards the thioenolimine or thioenolenamine form. Mass spectra of differently substituted enaminones are examined looking for common mass spectral behaviors. Ion fragmentations from specific tautomers allow predicting the most stable structure for the selected compounds. Acceptable correlation between the experimental data and theoretical results are found only with the neutral species, indicating that mass spectrometry could be resourced as a tool for the investigation of tautomerism of neutral species in the gas phase.

1. Introduction

Q4

Enaminones are a group of organic compounds derived from β-diketones, β-keto esters or other compounds containing a β-dicarbonyl moiety and the conjugated system C=C–C=O. The chemistry of enaminones is a developing field in organic synthesis [1,2]. These compounds are versatile synthetic intermediates that combine the ambident nucleophilicity of enamines with the ambident electrophilicity of enones [3]. There are many reports on functionalization of enaminone in the literature by the introduction of different substituents on the nitrogen, the α-carbon and the β-carbonylic carbon atoms. These derivatives have been extensively used for the preparation of a variety of heterocyclic systems some natural products and their analogues [4–6]. The enaminones are very useful synthetic intermediates in the preparation of biologically active heterocycles [7–9], including anticonvulsants [10], and anti-inflammatory [11] and anticancerous [12].

The open-chain enaminones have proven to be excellent prodrug of primary amines primarily by its ability to transport across biological membranes, while some cyclical enaminones are effective antiepileptic agents that act as blockers of the sodium channel conduction in nerve cells [13].

Understanding the mechanism of many reactions and biochemical processes, including those involving specific interactions with proteins, enzymes, and receptors (in which a substrate or active intermediary tautomerizes), requires a comprehensive understanding of the tautomerization process.

Tautomerism has an important role in biological system and has been actively investigated by many researchers. For example, the origin of serious DNA mutation is regarded as keto-enol and/or amine–imine tautomerisms [14–17].

It has been demonstrated in the case of keto-enol tautomerism of a variety of carbonylic and thiocarbonylic compounds [18–24], that there is no significant interconversion of the tautomeric forms in the gas phase following electron impact ionization in the mass spectrometer (molecular ions, $M^{+\bullet}$, do not seem to undergo unimolecular tautomerization) and, even more surprising, for GC/MS experiments, once the solvent is separated after injection in the injection port of the gas chromatograph, tautomerism mechanisms would not seem to take place even with no GC separation (under the selected experimental conditions). These conclusions are supported by temperature studies at the ion source (negligible effect) and at the injection port of the gas chromatograph with a shifting effect in agreement with the corresponding heats of tautomerization [18,23,24]. In fact, this process would take place very fast under the working conditions in the GC.

Separation of tautomers in the analytical column are frequently very difficult, consequently the different pathways of

Q2 * Corresponding author. Tel.: +54 2214243104.
E-mail address: pallegre@quimica.unlp.edu.ar (P.E. Allegretti).

http://dx.doi.org/10.1016/j.ijms.2014.12.010
1387-3806/

fragmentation of the tautomeric forms have to be used for identification of individual tautomers. For this reason and because of the high similarity between MS (commercial databases) and GC/MS spectra, analytical separation has not been considered critical for the present work. Analogously, it is thought that most of the conclusions could be useful to analyze spectra registered with mass spectrometers equipped with direct insertion probes.

This work, the study tautomeric equilibria spectrometric present in selected enaminones has been carried out, using mass spectrometry as a predictive tool.

2. Materials and methods

2.1. Synthesis of enaminones

Not commercially available enaminones were synthesized and purified according to literature procedures, by condensation of β-dicarbonyl compounds with primary or secondary amines in refluxing toluene followed by azeotropic removal of water [25,26].

The compounds under study were identified by NMR (^{1}H and ^{13}C) (Table 1, Supplementary information).

2.2. Gas chromatography–mass spectrometry—Single quadrupole

These determinations were performed by injection of methanol solutions (1 μl, 0.1%) in an HP 6890 Chromatograph coupled to an HP 5972A mass selective detector. The analytical column was a HP5-MS (30 m × 0.25 mm × 5 μm) using Helium as carrier gas (0.6 ml/min). The temperatures set points were: 200 °C at the injector, 300 °C at the interface, 185 °C at the ion source and the oven ramp was 40 °C (5 min), 20 °C/min, 290 °C. The electron energy was 70 eV and the pressure in the mass spectrometer was low enough ($<10^{-5}$ torr) as to preclude ion-molecule reactions (no autoprotonation observed).

2.3. Gas chromatography–mass spectrometry—Ion trap

These determinations were performed by injection of methanol solutions (1 μl) in a Thermo Quest Trace 2000 coupled to Finnigan Polaris ion trap detector (unit mass resolution) under the same experimental conditions already mentioned for the single quadrupole GC/MS system. This instrumentation was utilized to confirm proposed fragmentation pathways by CID (collision induced dissociation) using Helium as the damping gas, a CID voltage of 5–7 eV and an excitation energy of 0.35–0.45 eV (values were optimized for each ion transition). These experiments were done by selecting a precursor ion from the full-scan spectrum and carrying out the corresponding MS/MS product ion scan (Tables 1–4).

Table 1
MS2 data for 4-amino-2-penten-2-one (**I**).

Precursor ion (*m*/*z*)	Relevant product ions (*m*/*z*)
99	81, 82, 84
84	56, 57, 66
82	67, 40

Table 2
MS2 data for 3-amino-1-phenyl-2-butenone (**II**).

Precursor ion (*m*/*z*)	Relevant product ions (*m*/*z*)
161	160, 145, 144, 143, 120, 105, 84
120	102
105	77

Table 3
MS2 data for 4-phenylamine-3-penten-2-thione (**VIII**).

Precursor ion (*m*/*z*)	Relevant product ions (*m*/*z*)
191	176, 158, 157, 130, 118, 114, 99, 93, 59
158	143
157	142

Table 4
MS2 data for 4-dimethylamino-3-buten-2-one **(IX)**.

Precursor ion (*m*/*z*)	Relevant product ions (*m*/*z*)
113	98, 96, 43
70	55

2.4. Magnetic nuclear resonance determinations

^{1}H NMR spectra in $CDCl_3$, were recorded with a Varian Mercury Plus spectrometer operating at 4.7 T. The typical spectral conditions were as follows: spectral width 3201 Hz, acquisition time 4.09 s and 16 scans per spectrum. Digital resolution was 0.39 Hz per point. Deuterium from the solvent was used as the lock and TMS as the internal standard. Sample concentration was 20 mg/ml in deuterated chloroform. Measurements were performed at 25 °C.

^{13}C proton decoupled and gated decoupled spectra were recorded with the same spectrometer from $CDCl_3$ solutions at 25 °C. The spectral conditions were as follows: spectral width 10,559 Hz, acquisition times 1.303 s and 1000 scans per spectrum. Sample concentration was 40 mg/ml in deuterated chloroform and digital resolution was 1.29 Hz per point.

A standard one-dimensional (1D) proton NMR spectrum and a carbon spectrum with broad-band proton decoupling were run of each sample, supplemented by 2D gradient-selected COSY and multiplicity-edited HSQC experiments to help with the assignment of signals. All 2D spectra were recorded with the same spectrometer.

Vendor provided pulse sequences were used throughout the work.

2.5. Theoretical calculations

There are several computational procedures for treating tautomeric equilibria, being density functional theory (DFT) methods [27] dominant over the last few decades. Given the enormous number of available functionals, the prediction of the tautomerism by quantum chemistry depends strongly on the DFT functional and basis set used [28].

All tautomers of compounds under study were subjected to geometry optimizations using the DFT. In order to aim this, B3LYP hybrid exchange-correlation functional [29] together with the 6-31G(d,p) basis set as implemented in the Gaussian 03 package [30] was used. Numerous conformations were computed in order to ensure that the lowest energy conformation was obtained for each molecular system. All geometrical parameters were optimized without constraints.

3. Results and discussion

The relevance of spectrometric data as a predictive tool in regard to tautomeric equilibria depends mainly on the fact that the contribution due to tautomerization of molecular ions in the gas phase does not take place or can be ignored. The importance of this point comes from the physicochemical properties of radical ions that can be quite different from the neutral species. This could be the reason of possible distortion of results and loss of the desirable predictive power of the methodology. In fact, based on previous success

Please cite this article in press as: D.L. Ruiz, et al., Int. J. Mass Spectrom. (2015), http://dx.doi.org/10.1016/j.ijms.2014.12.010

to find good correlations, complex thermo dynamical discussions on fragmentations and rearrangements are out of the scope of this work. Since temperature effects are relevant to the determination of enthalpy differences, both sample introduction system (GC) and ion source (MS) temperatures were modified to find evidence regarding the involvement of neutral or ionic species in the spectrometric results produced by tautomerism occurrence. For the studied compounds, no significant changes are observed when modified the ion source temperature (data not shown).

It has been demonstrated in the case of keto-enol tautomerism of a variety of carbonyl and thiocarbonyl compounds [20–24], that there is no significant interconversion of the tautomeric forms in the gas phase following electron impact ionization in the ion source of the mass spectrometer prior to fragmentation (molecular ions, $M^{+\bullet}$, do not seem to undergo unimolecular tautomerization). Besides, for GC/MS experiments, once the solvent is separated after injection in the injection port of the gas chromatograph, tautomerism mechanisms (intermolecular or unimolecular) would not seem to take place even with no GC separation of the tautomers (under the selected experimental conditions). These conclusions are supported by temperature studies at the ion source (negligible effect) and at the injection port of the gas chromatograph (shifts of the relative abundances of tautomer-specific ions are in agreement with the corresponding heats of tautomerization) [22,24]. In fact, tautomerism would take place very fast in the injection port of the GC under the working conditions.

The present study involves a series of enaminones with diverse substitution. Not only the electronic effects of the substitution (electron-donating and withdrawing substituents) are analyzed but also the effects of substituent size are considered. In order to support the fact that tautomerism does not take place after ionization, we have also analyzed tautomerism of a methylated model compound by means of mass spectrometry. The selected compound was 4-methoxy-penta-2,4-dien-2-amine.

In order to support the fact that tautomerism does not take place after ionization, we have also analyzed tautomerism of a methylated model compound by means of mass spectrometry. Synthesis was performed of 4-methoxy-penta-2,4-dien-2-amine, the corresponding methylated enol of 4-amino-3-penten-2-one.

Separation of the tautomers in the analytical column are usually very difficult, consequently, the different pathways of fragmentation of the tautomeric forms have to be used for identification of individual tautomers [18]. For this reason and because of the high similarity between MS (commercial databases) and GC/MS spectra (the GC separation would not contribute to the complex distribution of internal energies of the ions formed in the ion source), the analytical separation has not been considered critical for the present work. Analogously, it is thought that most of the conclusions could be useful to analyze spectra registered with mass spectrometers equipped with direct insertion probes.

By the other hand, respecting separation of tautomers, even when it is very difficult in analytical columns it has been proven to occur in previous work in which we have separated β-ketoesters tautomers in chromatographic GC-columns [20].

Respecting the stability of ions and their effect on tautomerism, we are aware of the fact that ions from different compounds have different stability, but we assume that they have similar behavior given that they have similar structure. The usage of their abundances for estimating the trend in tautomerism is supported by previous studies made on many compounds families [18–24].

The present study involves a series of enaminones with diverse substitution. Not only the electronic effects of the substitution (electron-donating and withdrawing substituents) are analyzed but also the effects of substituent size are considered.

A detailed study of the mass spectra of selected enaminones was carried out, and fragmentation pathways for each tautomer were proposed to account for the specificity of their assignments.

Scheme 1 shows all the possible tautomeric structures for enaminones. The tautomeric forms that β-enaminones can show are: keto-enamine, keto-imine, enol-imine, and enol-enamine [7].

The most stable tautomeric forms are keto-enamine and enol-enamine (Table 2 Supplementary information), and they are the ones that could be analyzed using this methodology.

As an example, the mass spectrum of 4-amino-3-penten-2-one (**I**), 3-amino-1-phenyl-2-buten-1-one (**II**), ethyl-3-phenylamino-2-butenoate (**VII**), 4-phenylamino-3-penten-2-thione (**VIII**), and 4-dimethylamino-3-buten-2-one (**IX**) are shown.

Fig. 1 shows the mass spectrum of 4-amino-3-penten-2-one (**I**).

The ion at m/z 84, $(M{-}CH_3)^+$, is responsible of the base peak. This fragmentation can be assigned to all tautomers. The fragment ion at m/z 43 $(CH_3CO)^+$ and m/z 56 $(NH_2CH_2CH{=}C)^+$, cannot be assigned nor to enol-imine form neither to the enol-enamine form.

The ion at m/z 81 $(M{-}H_2O)^+$ can be considered as coming exclusively from the enol form (enol-imine or enol-enamine). Analogously, the ion at m/z 83, $(M{-}NH_2)^+$, can be explained from the keto-enamine or enol-enamine form. The ion at m/z 82 $(M{-}OH)^+$ could be due to the loss of OH (enol form) or NH_3 (which cannot be considered specific to the enamine form since it can be formed by Scheme 2 from the imine structure). The fragment ion at m/z 40 can be considered as coming from enolimine, keto-imine and keto-enamine forms.

The fragment ion at m/z 66 might be assigned to the enol (enol-enamine or enol-imine) form (Scheme 3).

Other ions are those at m/z 40, $(CH_2CCH_2)^{+\bullet}$, which could be explained from keto-enamine, keto-imine or enol-imine forms; the m/z 58, $(CH_2COHCH_3)^{+\bullet}$, and m/z 42, $(CH_2CNH_2)^+$, that could be explained from all tautomers.

The following fragmentation pathways were confirmed by GC–MS-Ion Trap experiments: the ions at m/z 81, 82 and 84 are generated from the molecular ion at m/z 99 and the ion at m/z 56, m/z 57 and m/z 66 from that one at m/z 84; the ion at m/z 40 from that one at m/z 82 (Table 1).

Fig. 2 shows the mass spectrum of 3-amino-1-phenyl-2-buten-1-one (**II**). In this case, the enol-imine, keto-enamine and keto-imine form can be considered.

When considering the mass spectrum of **II**, the following conclusions can be drawn:

The ions at m/z 160, $(M{-}H)^+$ (responsible of the base peak), m/z 146 $(M{-}CH_3)^+$; m/z 84 $(M{-}Ph)^+$, could be explained from all tautomers.

The m/z 105 $(PhCO)^+$ can come only from keto-enamine or keto-imine form and the m/z 145 $(M{-}NH_2)^+$ can be explained from the keto-enamine form.

The ion at m/z 144 could be explained as $(M{-}OH)^+$ from enol-imine form or as $(M{-}NH_3)^{+\bullet}$ from keto-enamine or keto-imine form.

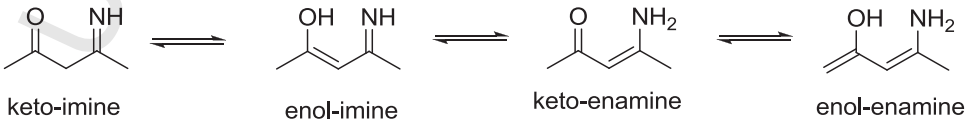

Scheme 1. Tautomers of enaminones.

Please cite this article in press as: D.L. Ruiz, et al., Int. J. Mass Spectrom. (2015), http://dx.doi.org/10.1016/j.ijms.2014.12.010

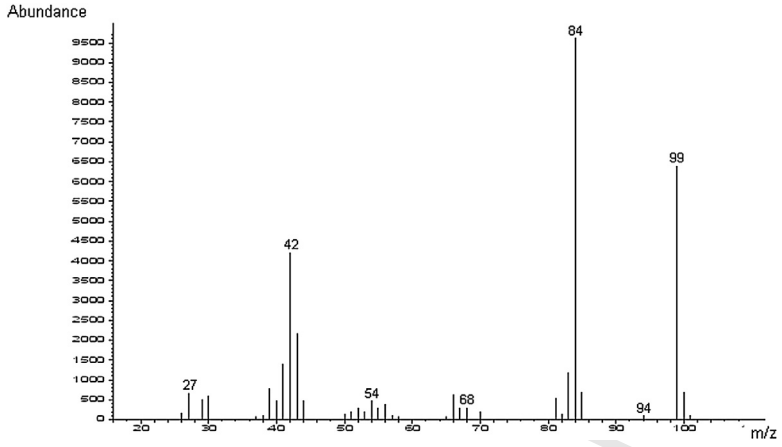

Fig. 1. Mass spectrum of 4-amino-3-penten-2-one (**I**).

The *m*/*z* 120 could be explained from the keto-imine form (Scheme 4).

The *m*/*z* 102 can come only from enol-imine form (Schemes 5 and 6). Scheme 6 depicts the formation of $(CH{=}CR)^{+\bullet}$ by loss of $CH_2{=}C{=}NR$ followed by loss of H_2O from the enol-imine form.

The following fragmentation pathways were confirmed by GC–MS-Ion Trap experiments: the ion at *m*/*z* 120 comes from that one at *m*/*z* 161 and the ion at *m*/*z* 102 from that one at *m*/*z* 120 (Table 2).

Fig. 3 shows the mass spectrum of ethyl-3-phenylamino-2-butenoate (**VII**).

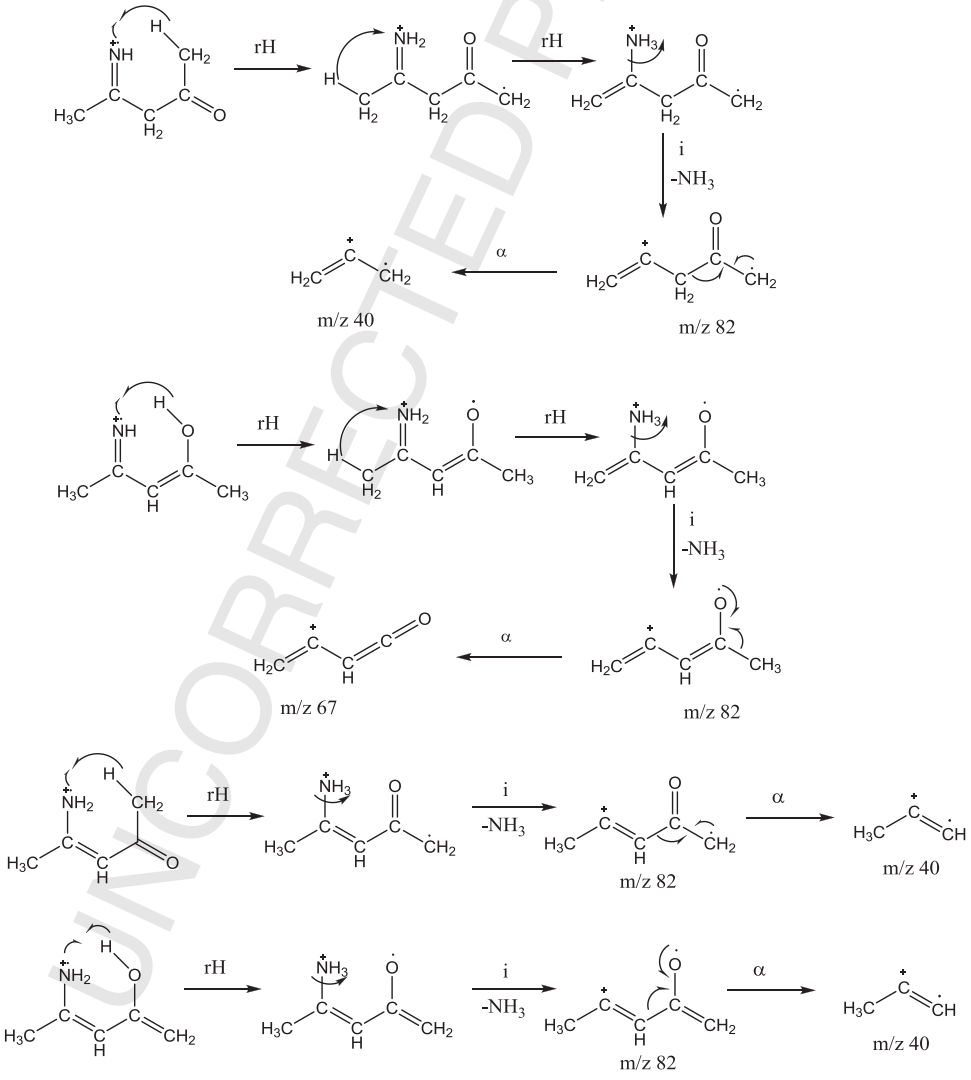

Scheme 2. Fragmentation pathway of 4-amino-3-penten-2-one.

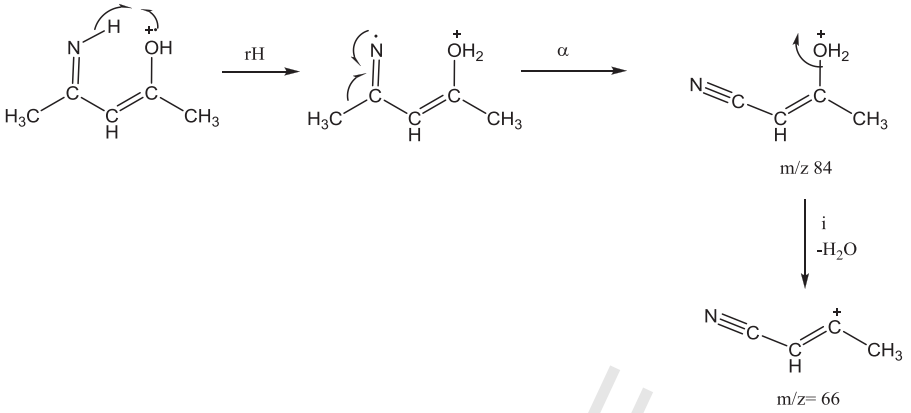

Scheme 3. Hydrogen rearrangement leading to ion *m*/*z* 66 in 4-amino-3-penten-2-one.

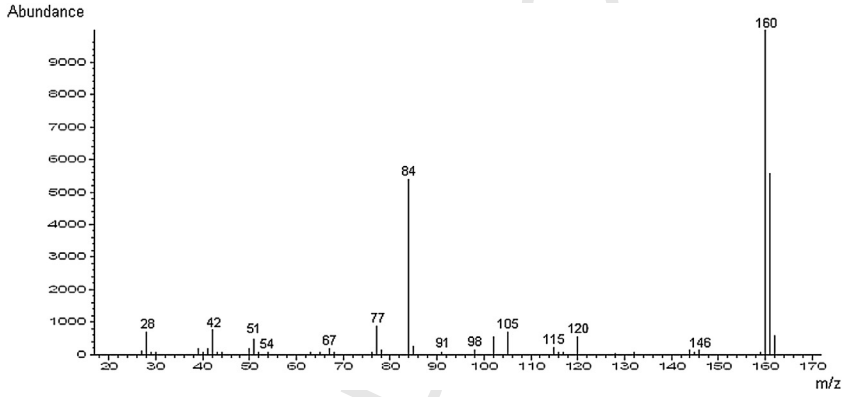

Fig. 2. Mass spectrum of 3-amino-1-phenyl-2-buten-1-one (**II**).

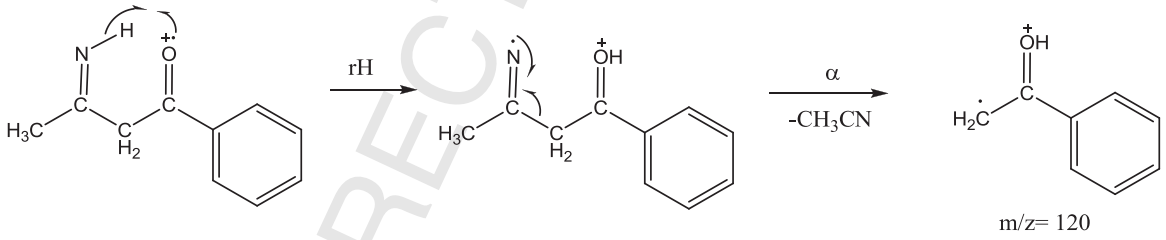

Scheme 4. Hydrogen rearrangement leading to ion *m*/*z* 120 from the keto-imine form in 3-amino-1-phenyl-2-buten-1-one.

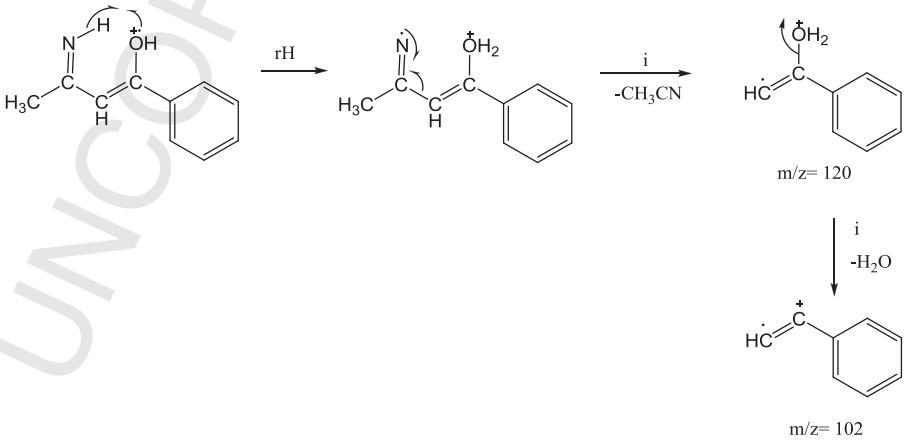

Scheme 5. Hydrogen rearrangement leading to ion *m*/*z* 102 from the enol-imine form in 3-amino-1-phenyl-2-buten-1-one.

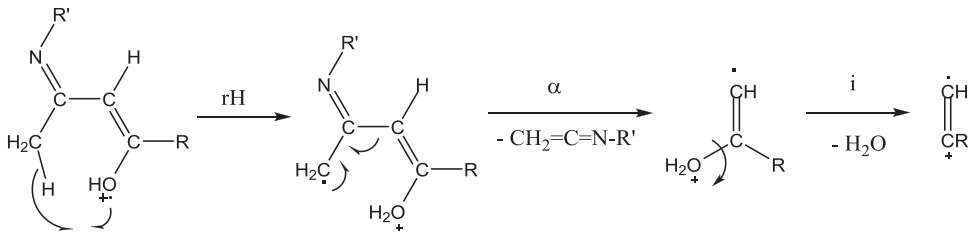

Scheme 6. Hydrogen rearrangement leading to ion $(CH{=}CR)^{+\bullet}$ from the enol-imine form in 3-amino-1-phenyl-2-buten-1-one.

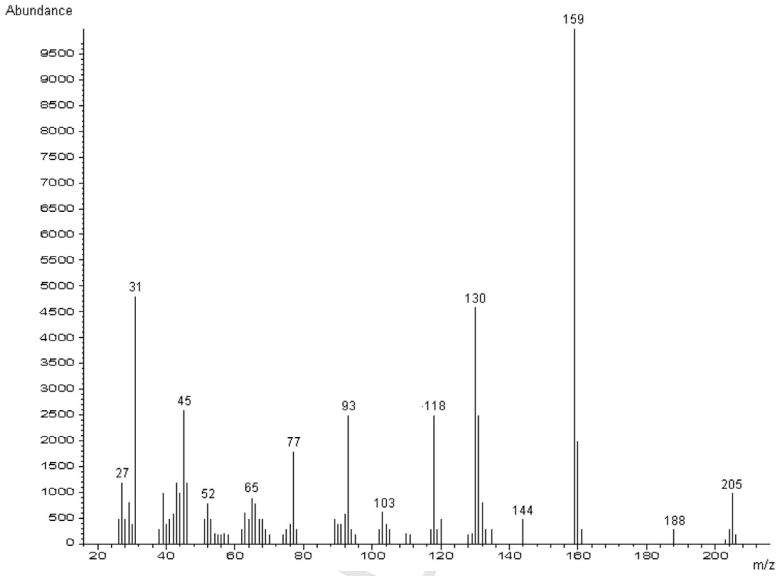

Fig. 3. Mass spectrum of ethyl-3-phenylamino-2-butenoate (**VII**).

The m/z 160 $(M{-}OCH_2CH_3)^+$; m/z 159 (base peak) $(M{-}HOCH_2CH_3)^{+\bullet}$; m/z 130 $(C_9H_8N)^+$ and m/z 118 $(Ph\ NC_2H_3)^+$ could be explained from all tautomers.

The ion at m/z 132 can be explained from the keto tautomer (keto-enamine or keto-imine form).

The ion at m/z 93 $(PhNH_2)^{+\bullet}$, m/z 113 $(M{-}PhNH)^+$ and m/z 112 $(CH_2{=}C{=}C{-}C(OCH_2CH_3){=}OH)^{+\bullet}$ can only be attributed to keto-enamine form.

The ion at m/z 188 $(M{-}OH)^+$ can be explained from the enol-imine form (enol-enamine form does not exist in this case). In this case, it cannot be due to loss of ammonia, as there is a phenyl group on the nitrogen.

Fig. 4 shows the mass spectrum of 4-phenylamine-3-penten-2-thione (**VIII**).

The base peak (m/z 114) corresponds to the loss of phenyl group from molecular ion and could be explained from all tautomers. In the same way, m/z 176 $(M{-}CH_3)^+$, m/z 93 $(PhNH_2)^{+\bullet}$, m/z 118 $(PhNHCHCH)^+$ and m/z 77 $(Ph)^+$ could be explained from all tautomers.

On the other hand, the m/z 118 can be explained from the imine form (thioketo or thioenol form).

The ion at m/z 158 $(M{-}SH)^+$ and m/z 157 $(M{-}SH_2)^{+\bullet}$ can be explained from thioenol form (enamine or imine form) and the ion at m/z 59 $(CH_3CS)^+$ can only be attributed to thioketo form (enamine or imine).

The m/z 99 $(CH_3C{=}CHCSCH_3)^+$ or $(CH_3C{=}CHCSH{=}CH_2)^+$ can be attributed to the enamine-thioketo or enamine-thioenol form.

The m/z 142 corresponds to the loss of SH_2 and methyl group from molecular ion. In the same way, m/z 143 could be explained by loss of the SH followed of methyl group, both peaks may be attributed to thioenol form.

The following fragmentation pathways were confirmed by GC–MS-Ion Trap experiments: the ions at m/z 176, 158, 157, 130, 118, 114, 99, 93 and 59 are generated from the molecular ion at m/z 177 and the ion at 143 from that one at m/z 158; the ion at m/z 142 from that one at m/z 157 (Table 3).

Fig. 5 shows the mass spectrum of 4-dimethylamine-3-buten-2-one (**IX**).

The importance of looking into this mass spectrum is that it can only exist as enamine allowing studies only keto-enol equilibrium (Scheme 7).

The base peak (m/z 98) corresponds to the loss of methyl group from molecular ion and could be explained from both tautomers. In the same way, m/z 44 and m/z 70 $(M{-}COCH_3)^+$ could be explained from both tautomers.

The ion at m/z 96 $(M{-}OH)^+$ can be explained from enol form, so that it is possible to conclude that the loss of 17 amu from the molecular ion observed for the previous enaminones also be due mostly to the loss of OH. The peak at m/z 68 corresponding to the loss of NH $(CH_3)_2^+$ indicates that a small percentage corresponds to the loss of NH_3.

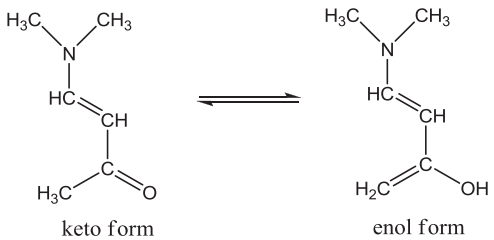

Scheme 7. Keto-enol equilibrium in 4-dimethylamino-3-buten-2-one.

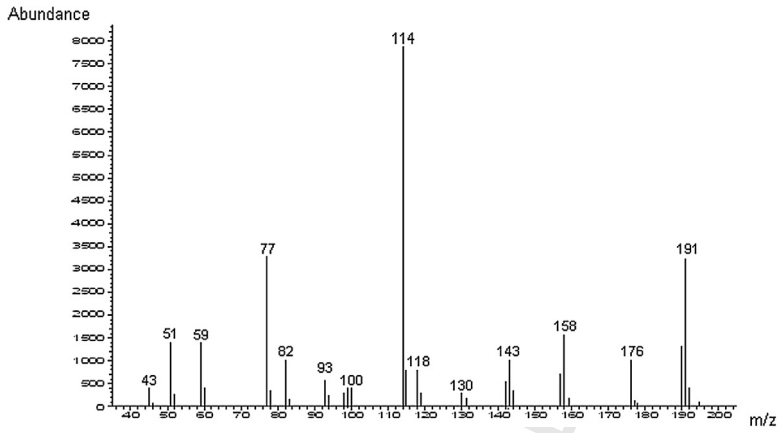

Fig. 4. Mass spectrum of 4-phenylamine-3-penten-2-thione (**VIII**).

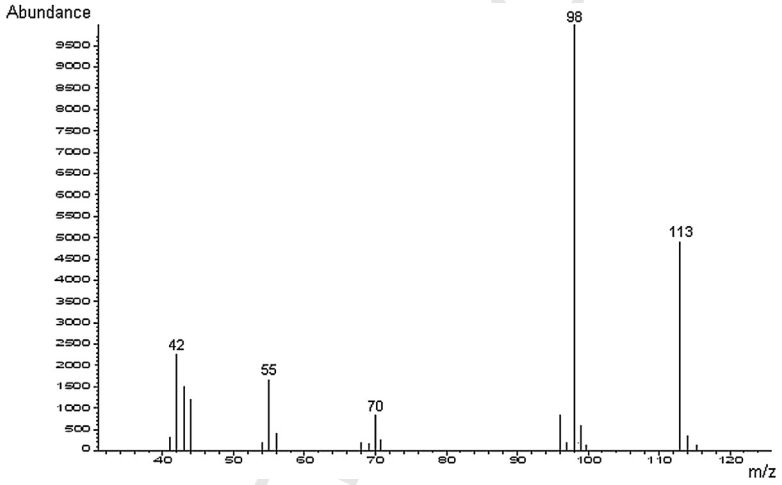

Fig. 5. Mass spectrum of 4-dimethylamine-3-buten-2-one (**IX**).

The ion at *m*/*z* 55 corresponds to the ($COCH_3$) loss from the molecular ion followed by loss of methyl group.

The ion at *m*/*z* 43 $(CH_3CO)^+$ can only be attributed to keto form.

The following fragmentation pathways were confirmed by GC–MS-Ion Trap experiments (Table 4): the ions at *m*/*z* 98, 96 and 43 are generated from the molecular ion at *m*/*z* 113 the ion at *m*/*z* 55 comes from that one at *m*/*z* 70.

Fig. 6 shows the mass spectrum of 4-methoxy-penta-2,4-dien-2-amine.

The ion at *m*/*z* 98 is responsible basis peak, as in the analogue.

The ions at *m*/*z* 82 $(M—OCH3)^+$ and *m*/*z* 81 $(M—CH_3OH)^{+\bullet}$ can be compared to the loss of OH and H_2O, respectively, for 4-amino-3-penten-2-one (peaks were assigned to the enol tautomer). Loss OCH_3 implies that the 4-amino-3-penten-2-one loss of 17 amu mostly corresponds to OH, with contribution NH_3 given that also the ion *m*/*z* 96 $(M—NH_3)^+$ observed.

The following fragmentation pathways were confirmed by GC–MS-Ion Trap experiments (Table 5).

Table 5
MS2 data for 4-methoxy-penta-2,4-dien-2-amine.

Precursor ion (*m*/*z*)	Relevant product ions (*m*/*z*)
113	112, 98, 97, 96, 82, 81, 57
96	65
81	66

Based on comprehensive review of the mass spectra of selected enaminones the fragmentations as indicated in Schemes 6 and 8 can be generalized.

Scheme 8 depicts the formation of $(RN{=}C{=}CH{-}C{=}CH_2)^+$ by loss of CH_3 followed by loss of water from the enol-enamine form. As observed, this fragmentation pathway proposal is only possible in the case of the compounds 4-amino-3-penten-2-one (**I**), 4-methylamino-3-penten-2-one (**IV**), 4-phenylamino-3-penten-2-one (**V**) and 4-phenylamino-3-penten-2-thione **(VIII)**.

The loss of 17 or 33 uma y el $[M{-}CH_3{-}H_2O/H_2S]^+$ may be attributed to enol or thioenol form.

The ion $[RCO]^+$ can be explained from keto form. It is not possible to attribute specific peaks for imine or enamine form.

The fragment ion $(CH{=}CR)^{+\bullet}$ may be attributed to enol-imine form.

Table 6 shows the relevant mass spectral data for selected enaminones.

The reported electron impact ion abundances were calculated according to the following ratio:

$$\frac{\text{Ion abundance} \times 1000}{\sum \text{abundances}}.$$

Since coexisting tautomers are not separated by chromatography in these conditions, the mass spectra are the result of mass spectra superposition, so that accurate fragments should be selected for proper comparison.

Please cite this article in press as: D.L. Ruiz, et al., Int. J. Mass Spectrom. (2015), http://dx.doi.org/10.1016/j.ijms.2014.12.010

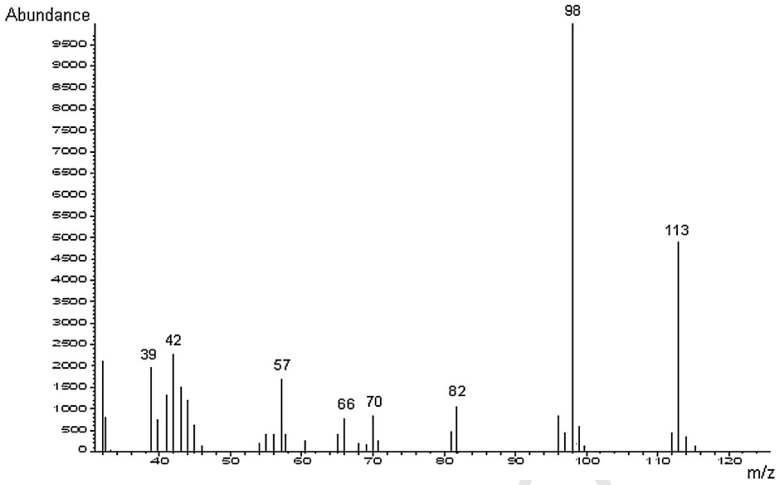

Fig. 6. Mass spectrum of 4-methoxy-penta-2,4-dien-2-amine.

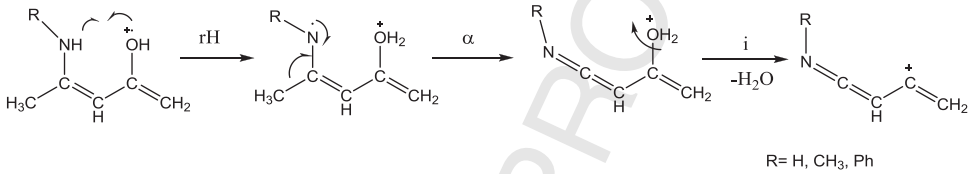

Scheme 8. Formation of $(RN{=}C{=}CH{-}C{=}CH_2)^+$ from the enol-enamine form in **I**, **IV**, **V** and **VIII**.

As it can be observed, the equilibrium position depends on the substituent nature regarding electronic and steric effects [31,32].

By analyzing 4-amino-3-penten-2-one (**I**) and 3-amino-1-phenyl-2-buten-1-one (**II**), the enol content in the gas phase is **II** > **I**, which is explainable in electronic (extent of conjugation in **II**) and steric terms (1.1 vs 1.0 for the ratio $[(M{-}OH)^+]/[(RCO)^+]$ or 3.0 vs 0.8 for the ratio $[(CH{=}CR)^{+\bullet}]/[RCO^+]$. Furthermore, as can be expected, the ester function has no evidence of the enol-imine form, ethyl 3-amino-2-butenoate (**III**) vs 4-amino-3-penten-2-one (**I**) (0.1 vs 1.0 for the ratio $[(M{-}OH)^+]/[RCO^+]$ or 0.7 vs 0.8 for the ratio $[(CH{=}CR)^{+\bullet}]/[RCO^+]$; ethyl 3-(methylamino)-2-butenoate (**VI**) vs 4-(methylamino)-3-penten-2-one (**IV**) (1.0 vs 1.1 for the ratio $[(M{-}OH)^+]/[RCO^+]$ or 1.5 vs 4.3 for the ratio $[(CH{=}CR)^{+\bullet}]/[RCO^+]$ and ethyl 3-(phenylamino)-2-butenoate (**VII**) vs 4-(phenylamino)-3-penten-2-one (**V**) (1.5 vs 4.1 for the ratio $[(M{-}OH)^+]/[RCO^+]$ or 3.6 vs 5.2 for the ratio $[(CH{=}CR)^{+\bullet}]/[RCO^+]$.

Comparing 4-(methylamino)-3-penten-2-one (**IV**) vs 4-amino-3-penten-2-one (**I**) (1.1 vs 1.0 for the ratio $[(M{-}OH)^+]/[RCO^+]$ or 4.3 vs 0.8 for the ratio $[(CH{=}CR)^{+\bullet}]/[RCO^+]$; 4-(phenylamino)-3-penten-2-one (**V**) vs 4-amino-3-penten-2-one (**I**) (4.1 vs 1.0 for the ratio $[(M{-}OH)^+]/[RCO^+]$ or 5.2 vs 0.8 for the ratio $[(CH{=}CR)^{+\bullet}]/[RCO^+]$ and 3-(methylamino)-2-butenoate (**VI**) vs ethyl 3-amino-2-butenoate (**III**) (1.0 vs 0.1 for the ratio $[(M{-}OH)^+]/[RCO^+]$ or 1.5 vs 0.7 for the ratio $[(CH{=}CR)^{+\bullet}]/[RCO^+]$ ethyl 3-(phenylamino)-2-butenoate (**VII**) vs ethyl 3-(methylamino)-2-butenoate (**VI**) (1.5 vs 1.0 for the ratio $[(M{-}OH)^+]/[RCO^+]$ or 3.6 vs 1.5 for the ratio $[(CH{=}CR)^{+\bullet}]/[RCO^+]$ shows that the imino-enol is more stable in the case of *N*-substituted enaminones.

For *N*-methylsubstituted vs *N*-phenylsubstituted, both the size of the substituents and the additional stabilization by the extended conjugation of the corresponding enol are relevant: 4-phenylamino-3-penten-2-one (**V**) vs 4-methylamino-3-penten-2-one (**IV**) (4.1 vs 1.1 for the ratio $[(M{-}OH)^+]/[RCO^+]$ or 5.2 vs 4.3 for the ratio $[(CH{=}CR)^{+\bullet}]/[RCO^+]$, and ethyl 3-phenylamino-2-butenoate (**VII**) vs ethyl 3-methylamino-2-butenoate (**VI**) (1.5 vs 1 for the ratio $[(M{-}OH)^+]/[RCO^+]$ or 3.6 vs 1.5 for the ratio $[(CH{=}CR)^{+\bullet}]/[RCO^+]$.

On the other hand, as can be seen, with the exchange in heteroatom (O—S) a strong equilibrium shift towards the enol tautomer is observed: 4-phenylamino-3-penten-2-thione (**VIII**) vs 4-phenylamino-3-penten-2-one (**V**) (10.0 vs 4.1 for the ratio $[(M{-}SH)^+]/[RCO^+]$ or 11.7 vs 5.2 for the ratio $[(CH{=}CR)^{+\bullet}]/[RCO^+]$.

The thione group is relatively unstable in the monomeric form and tends to turn into a stable C—S single bond [33]. As already established in previous work, the heteroatom O—S exchange causes a noticeable effect on the equilibrium position [34,35]. Thus, aliphatic thioketones exist in equilibrium with their enethiols [35].

Table 6
Relevant mass spectral data for selected enaminones (X = O or S).

Compound	M+•	$[M{-}XH]^+$	$[CH{=}CR]^{+\bullet}$	$[R{-}CO]^+$	$[M{-}XH]^+/[RCO]^+$	$[CH{=}CR]^{+\bullet}/[RCO]^+$
I	198	3.0[A]	2.4	3.0	1.0	0.8
II	191	10.8[A]	30.6	10.2	1.1	3.0
III	41	0.2	1.5	2.1	0.1	0.7
IV	188	25.0	94.2	21.9	1.1	4.3
V	110	21.1	21.1	5.2	4.1	5.2
VI	64	2.4	3.6	2.4	1.0	1.5
VII	22	6.5	15.5	4.3	1.5	3.6
VIII	163	116.6	136.9	11.7	10.0	11.7

[A] It may be due to loss of OH or NH_3.

Scheme 9. Resonance structure of thiocarbonylic compounds.

Table 7
Calculated enolimine–ketoenamine heats of formation differences for the selected molecules and corresponding molecular ions.

Compound	$\Delta\Delta E \pm 2$ kJ/mol neutral molecule	$\Delta\Delta E \pm 2$ kJ/mol molecular ion
I	42.5	22.9
II	35.5	34.8
III	46.9	40.8
IV	44.6	38.4
V	33.2	18.2
VI	58.3	22.5
VII	39.8	19.9
VIII	22.5	34.6

This results arised from the greater polarization of the thiocarbonyl group (Scheme 9) (i.e. greater contribution of the canonical form b) when compared with carbonyl group, because of the greater difficulty of the larger sulfur atom to form π-bonds with carbon [36,37].

This effect seems to outweigh the greater electronegativity of oxygen [37].

Notwithstanding, to support that the observed tautomeric equilibria distributions come from the molecular species with negligible contribution from tautomerism of molecular ions, theoretical calculations of heats of formation were carried out for both species.

Table 7 also shows the enolimine–ketoenamine heats of formation differences for the selected molecules and corresponding molecular ions obtained from theoretical calculations.

A reasonable good correlation with the mass spectra observations is achieved only in the case of the neutral molecule (**II** vs **I**: 35.5 vs 42.5; **III** vs **I**: 46.9 vs 42.5; **IV** vs **I**: 44.6 vs 42.5; **V** vs **I**: 33.2 vs 42.5 and **VIII** vs **V**: 22.5 vs 42.2) When considering the radical ion not only there is no correlation with the experimental data but also no logical tendencies are observed (e.g. compare **II** vs **I**: 34.8 vs 22.9 and **VIII** vs **V**: 34.6 vs 18.2).

Then these findings are consistent with the tautomerism occurrence for the neutral species, before ionization, so that tautomerization after ionization in the ion source, if it occurs at all, has a negligible effect on the position of the equilibrium. This would be another indication giving support to the usefulness of mass spectrometry to predict tautomeric equilibria in the gas phase.

The sample introduction system temperature has been modified of selected compounds (compounds **I** to **V**). Experimental determinations are done independently by triplicate.

Eq. (1) provides a simple method to determine the heat of keto-enol tautomerization for the studied compounds.

$$\ln K = \frac{\ln[\text{enol} - \text{imine}]}{[\text{keto} - \text{enamine}]} = \frac{\ln[\text{f enol} - \text{imine}]}{[\text{f keto} - \text{enamine}]} = \frac{-\Delta H}{RT} + C \quad (1)$$

where [f enol-imine] and [f keto-enamine] are the abundance of the fragments corresponding to the enol-imine and keto-enamine forms, assuming that the concentration ratios are proportional to the ion fragment abundance ratios. Theoretical calculations support that the keto-enamine is much more stable than the imine-keto form, RCO^+ fragment was considered for calculating the equilibrium constant derived from the keto-enamine form.

Fig. 7 shows the representation of $\ln K$ vs $1/T$ for selected compounds.

The calculated slopes from Fig. 7 can be used directly to determine the enthalpy changes according to Eq. (1) (Table 8).

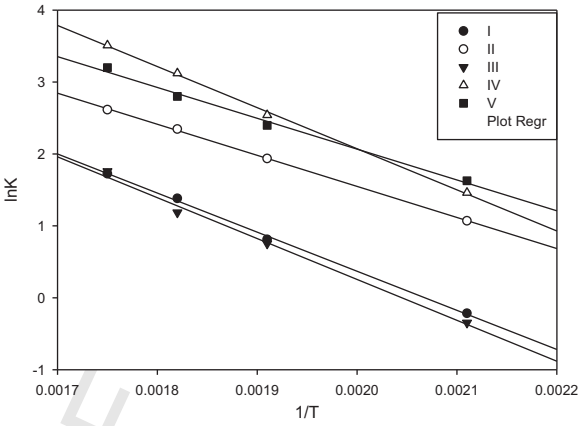

Fig. 7. Plot $\ln K$ vs $1/T$.

Table 8
Calculated slopes from Fig. 7 and enthalpy changes according to Eq. (1).

$y = ax + b$	Value	Standard error	R^2	ΔH (kJ/mol)
I Intercept	11.1	0.4	0.996	43.4
Slope	−5340	199		
II Intercept	10.1	0.2	0.997	35.3
Slope	−4246	126		
III Intercept	11.5	0.5	0.995	46.5
Slope	−5598	239		
IV Intercept	13.3	0.3	0.997	46.7
Slope	−5615	170		
V Intercept	10.5	0.4	0.993	35.1
Slope	−4219	201		

Table 9
Correlation between the heats of tautomerization calculated from the slopes of Fig. 7 and those determined by quantum chemical calculation.

Compound	Heat of tautomerization obtained from the slopes $\Delta E \pm 2$ (kJ/mol)	Heat of tautomerization from DFT calculations $\Delta E \pm 2$ (kJ/mol)
I	43.4	42.5
II	35.3	35.5
III	46.5	46.9
IV	46.7	54.6
V	35.1	42.2

The correlation between the heats of tautomerization calculated from the slopes of Fig. 7 and those determined by quantum chemical calculations is very good (Table 9), which provides strong support for the experimental data, proving once again that the spectrometry mass is a useful tool for calculating heats of tautomerization.

4. Conclusions

The mass spectra of some enaminones can provide valuable information regarding the ketoenamine–enolimine equilibria taking place in the gas phase (fast tautomerization equilibrium at the injection port of the gas chromatograph). The predictive value of this methodology is supported by the influence of the nature and size of substituents on tautomeric equilibria and the rather good correlation existing between the abundance ratios of selected fragments. Mass spectrometry seems to be useful in determining the most stable tautomer for selected enaminones and thioenaminones. Taking into consideration previous mass spectral and

molecular orbital calculations done on enaminones, the present studies allow to predict that the keto-enamine structure are particularly stable for enaminones and while the enol-enamine structure would predominate for thioenaminones. It seems that this observation accounts for the different nature of the carbonyl groups in the molecule.

It has been shown that the sensible employment of these two different methods enables one to achieve a predictive capability to study the tautomerization effect of the compounds under consideration in this work. The value of mass spectrometry as a tool to predict the occurrence of tautomerism has been demonstrated.

Acknowledgements

Q5 We are indebted to the Facultad de Ciencias Exactas, Universidad Q6 Nacional de La Plata for financial support, to Agencia Nacional de Promoción Científica y Tecnológica, República Argentina and the Consejo Nacional de Investigaciones Científicas y Tecnológicas.

Appendix A. Supplementary data

Supplementary data associated with this article can be found, in the online version, at http://dx.doi.org/10.1016/j.ijms.2014.12.010.

References

[1] A.A. Elasser, A.A. El-Khair, Tetrahedron 59 (2003) 84.
[2] S.M. Riyadh, I.A. Abdelhamid, H.M. Al-Matar, N.M. Hilmy, M.H. Elnagdi, Heterocycles 75 (2008) 1849.
[3] J.V. Greenhill, Chem. Soc. Rev. 6 (1977) 277.
[4] P. Lue, J.V. Greenhill, in: A.R. Katritzky (Ed.), Advances in Heterocyclic Chemistry, vol. 67, Academic Press, New York, NY, 1997, pp. 207–343.
[5] P.G. Baraldi, A. Barco, S. Benetti, G.P. Pollini, D. Simoni, Synthesis 1987 (10) (1987) 857.
[6] A.A. Hassan, Int. J. Org. Chem. 4 (2014) 68.
[7] V. Kuckländer, in: Z. Rappoport (Ed.), The Chemistry of Enamines, Part 1, John Wiley & Sons, New York, NY, 1994, pp. 525–639.
[8] M.A. El-Apasery, S.M. Al-Mousawi, H. Mahmoud, M.H. Elnagdi, Int. Res. J. Pure Appl. Chem. 1 (3) (2011) 69.
[9] D.E. Natalie, S.C. Donna, M. Khurana, N.S. Noha, P.S. James, J.H. Sylvia, N. Abraham, S.T. Robert, A.M. Jacqueline, Eur. J. Med. Chem. 38 (2003) 49.
[10] G. Dannhardt, A. Bauer, U. Nowe, J. Prakt. Chem. 340 (1998) 256.
[11] A.S. Shawali, J. Chem. Res. 34 (2010) 630.
[12] I.O. Edafiogho, O.A. Phillips, E.E. Udo, S. Samuel, B. Rethish, Eur. J. Med. Chem. 44 (2009) 967.
[13] M. Rueda, F.J. Luque, J.M. López, M. Orozco, J. Phys. Chem. A 105 (2001) 6575.
[14] G.J. Fogarasi, Phys. Chem. A 106 (2002) 1381.
[15] L.M. Salter, G.M. Chaban, J. Phys. Chem. 106 (2002) 4251.
[16] C.E. Crespo-Hernández, B. Cohen, P.M. Hare, B. Kohler, Chem. Rev. 104 (2004) 1977.
[17] P.B. Terent'ev, A.G. Kalandarishvili, K.N. Zelenin, O.V. Solod, V.K. Shevtsov, Chem. Heterocycl. Comp. 33 (9) (1997) 1070.
[18] P.E. Allegretti, C.B. Milazzo, J.J.P. Furlong, Eur. J. Mass Spectrom. 11 (2005) 53.
[19] P.E. Allegretti, M.M. Schiavoni, C. Guzmán Sampay, A. Ponzinibbio, J.J.P. Furlong, Eur. J. Mass Spectrom. 3 (2007) 291.
[20] P.E. Allegretti, M.M. Schiavoni, H.E. Di Loreto, J.J.P. Furlong, C.O. Della Védova, J. Mol. Struct. 560 (2001) 327.
[21] H. Saraví Cisneros, S.L. Laurella, D.L. Ruiz, P.E. Allegretti, J.J.P. Furlong, Int. J. Spectrosc. 2009 (2009) 18 (Article ID 408345).
[22] J.M. Giussi, B. Gastaca, A.G. Albesa, M.S. Cortizo, P.E. Allegretti, Spectrochim. Acta A: Mol. Biomol. Spectrosc. 78 (2011) 868.
[23] D.L. Ruiz, M.M. Schiavoni, S.L. Laurella, J.M. Giussi, J.J.P. Furlong, P.E. Allegretti, Spectrochim. Acta A: Mol. Biomol. Spectrosc. 78 (2011) 1397.
[24] H. Saraví Cisneros, M. Erben, C.O. Della Védova, S.L. Laurella, P.E. Allegretti, J.J.P. Furlong, Eur. J. Mass Spectrom. 17 (2) (2011) 125.
[25] P.G. Baraldi, D. Simoni, S. Manfredini, Synthesis 11 (1983) 902.
[26] C.K.Z. Andrade, A.F.S. Barreto, W.A. Silva, Arkivoc 12 (2008) 226.
[27] R.G. Parr, W. Yang, Density Functional Theory of Atoms and Molecules, Oxford University Press, New York, NY, 1989.
[28] W.M.F. Fabian, in: L. Antonov (Ed.), Tautomerism: Methods and Theories, Wiley-VCH Verlag GmbH & Co. KGaA, Weinheim, Germany, 2014 (Chapter 13).
[29] A.D. Becke, J. Chem. Phys. 98 (1993) 5648.
[30] M.J. Frisch, G.W. Trucks, H.B. Schlegel, G.B. Scuseria, M.A. Robb, J.R. Cheeseman, J.A. Montgomery Jr., T. Vreven, K. Kudin, J. Burant, J. Millam, S. Iyengar, J. Tomasi, V. Barone, B. Mennucci, M. Cossi, G. Scalmani, N. Rega, G. Petersson, H. Nakatsuji, M. Hada, M. Ehara, R. Toyota, R. Fukuda, J. Hasegawa, M. Ishida, T. Nakajima, Y. Honda, O. Kitao, H. Nakai, M. Klene, X. Li, J. Knox, H. Hratchian, J. Cross, C. Adamo, J. Jaramillo, R. Gomperts, R. Stratmann, A. Yazyev, R. Austin, C. Cammi, J.W. Pomelli, P.Y. Ochterski, K. Ayala, G.A. Morokuma, P. Voth, J.J. Salvador, V.G. Dannenberg, S. Zakrzewski, A.D. Dapprich, M.C. Daniels, O. Strain, D.K. Farkas, A.D. Malick, K. Rabuck, J.B. Raghavachari, J.V. Foresman, Q. Ortiz, A.G. Cui, S. Baboul, J. Clifford, B.B. Cioslowski, G. Stefanov, A. Liu, P. Liashenko, I. Piskorz, R.L. Komaromi, D.J. Martin, T. Fox, M.A. Keith, C.Y. Al-Laham, A. Peng, M. Nanayakkara, P.M.W. Challacombe, B. Gill, W. Johnson, M.W. Chen, C. Wong, R. Gonzalez, J.A. Pople, Gaussian 03, Revision B.03, Gaussian, Inc., Pittsburgh, PA, 2003.
[31] P.B. Terent'ev, A.G. Kalandarishvili, Mass Spectrom. Rev. 15 (1996) 339.
[32] R.L. Jarvest, I.L. Pinto, S.M. Ashman, G.E. Dabrowski, A.V. Fernandez, L.J. Jenning, P. Lavery, D.G. Tew, Bioorg. Med. Chem. Lett. 1999 (1999) 443.
[33] M.J. Janssen, Organosulfur Chemistry: Reviews of Current Research, Interscience Publisher, New York, NY, 1967.
[34] F.G. Bordwell, D.J. Algrim, J.A. Harrelson, J. Am. Chem. Soc. 110 (1998) 5903.
[35] S. Sklenak, Y. Apeloig, Z. Rappoport, J. Chem. Soc., Perkin Trans. 2 2 (2000) 2269.
[36] C.M. Lee, W.D. Kumler, J. Org. Chem. 27 (1962) 2052 (And references there cited).
[37] L. Pauling, The Nature of the Chemical Bond, third ed., Cornell University Press, Ithaca, NY, 1960, pp. 90.